JOURNAL OF MATERIALS SCIENCE **37** (2002) 3685–3691

Photochemistry of bistriphenyl phosphine nickel dicarbonyl on silicon surfaces: the lithographic deposition of nickel and nickel-iron, nickel-chromium and iron-chromium containing films

W. C. H. CHU, S. L. BLAIR, R. H. HILL
Department of Chemistry, Simon Fraser University, Burnaby, British Columbia, Canada, V5A 1S6
E-mail: ross@bohr.chem.sfu.ca

The photolysis of $Ni(CO)_2(PPh_3)_2$ as surface films on silicon surfaces has been investigated. The photolysis of the title complex leads to the loss of ligand from the coordination sphere and the formation of nickel. The ligands are largely lost to the gas phase although impurity originating from the triphenylphosphine ligand remains within the film. The controlled construction of films formed from a mixture of $Ni(CO)_2(PPh_3)_2$ and $Cr(CO)_5PPh_3$ could be accomplished by spin coating from a solution containing both precursors. Photolysis of films composed of a mixture of $Ni(CO)_2(PPh_3)_2$ and $Cr(CO)_5PPh_3$ resulted in the formation of a nickel-chromium film. In a similar fashion films constructed from of $Ni(CO)_2(PPh_3)_2$ and $Fe(CO)_4PPh_3$ could be photolysed to generate films of nickel-iron and films composed of $Cr(CO)_5PPh_3$ and $Fe(CO)_4PPh_3$ could be photolysed to generate films of chromium-iron. Both of these films contained impurities associated with remnant triphenylphosphine and oxidation of the surface. This process was shown to be compatible with standard lithography techniques by the lithography of 2 μm lines of triphenylphosphine contaminated nickel on a silicon surface.

1. Introdution

The use of organometallic compounds to generate metal and metal oxide materials has been demonstrated to occur by a variety of methods including both chemical vapor deposition (CVD) and the various photon enhanced CVD processes [1–9]. The advantage of the photon enhanced routes is the potential to use the photolysis to direct the deposition process. In applications where specific coating of limited areas is desirable, such as in the fabrication of microelectronic devices, such photon directed deposition is of potential importance. An additional advantage of the photochemical process is the low process temperature, which may be realized for photochemical processes. In many applications pure metals are not ideal and alloys of various metals are required. These mixtures are often chosen for a combination of properties including resistance toward diffusion into semiconductors, electronic properties, and adhesion. A variety of magnetic materials [10–12] are also composed of mixed transition metals and their oxides. In this paper we explore the utility of the surface photochemical method to fabricate films composed of more than one metal.

The deposition of alloys by gas phase photochemical deposition has been demonstrated [13]. In this process a change in the wavelength of irradiation could result in a change in the composition of the resultant alloy. The composition of the final deposited alloy was determined by a combination of the irradiation source and the concentration in the gas phase of the reactive species. The surface photochemical method is expected to have very different control parameters.

Here we present an alternate methodology for the fabrication of films composed of more than one metal. Previously we have demonstrated the ability to fabricate metal structures with a process of photolysis of films [14–22]. In this process an amorphous molecular film, cast by spin coating, is subjected to irradiation. This process may result in the formation of metals or metal oxides depending upon the reaction conditions. In this paper we explore the use of mixtures of organometallic complexes to generate amorphous films containing precursors to different transition metal centers. We expect the composition of the precursor films will control the composition of the resultant metal or metal oxide films. The entire film, once cast, should photochemically be convertible to a mixture of metals with no change in the amount of each metal. This is quite different from the gas phase control and hence may represent an attractive alternative in some applications. It should be

noted that we have used this process in the past to make ferroelectric materials such as PZT and BST [23, 24] from metalorganic precursors.

The complexes used in this study include metal carbonyl phosphines of some first row elements. The metals, nickel, iron and chromium, were chosen as a result of their application in magnetic materials. The metal carbonyl phosphines, $Ni(CO)_2(PPh_3)_2$, $Fe(CO)_4PPh_3$ and $Cr(CO)_5(PPh_3)$, were chosen since the similarity of the outer sphere should make the precursors easily form intimate mixtures on the surface. In addition the use of a large phosphine such as PPh_3 renders the vapor pressure low so evaporation of the complexes during the study will be inconsequential. A more practical consequence of this choice is that the complexes chosen are all reasonably air stable solids that are easily handled in air. In practice however this will have a negative impact on the final purity of the films in comparison without the lighter phosphines however our concern in this paper is more directed at the process investigation rather than the purity of the resultant material. Both the chromium and iron complexes have mechanisms which are somewhat complex and we have investigated these previously [15, 17]. The thin film photochemistry of the nickel complex we present here for the first time.

2. Experimental procedure

The silicon wafers were obtained from Pacific Microelectronics Center, Canada. The Si(111) surface was used in these studies and the wafers were p-type silicon with tolerances and specifications as per SEMI Standard M1.1.STD.5 cut to the approximate dimensions of 1 cm × 1.5 cm in house. The CaF_2 crystals were obtained from Wilmad Glass Co. Inc.. The nickel complex, $Ni(CO)_2(PPh_3)_2$, was obtained from Strem Chemical Co..

The FTIR spectra were obtained with 4 cm^{-1} resolution using a Bomem Michelson 120 FTIR spectrophotometer. The samples were held in an aluminum sample mount within either a NaCl or a CaF_2 faced vacuum dewar. The photolysis beam was a 100 W high pressure Hg lamp in an Oriel housing equipped with condenser lenses and filtered through a 10 cm water filter with quartz optics. Auger electron spectra were obtained using a PHI double pass CMA at 0.85 eV resolution at the Surface Physics Laboratory, Dept. of Physics, Simon Fraser University. Film thickness was determined using a Leitz Laborlux 12 ME S with an interference attachment.

2.1. Preparation of the complexes

The complexes, $Fe(CO)_4(PPh_3)$, $Fe(CO)_3(PPh_3)_2$, and $Cr(CO)_5(PPh_3)$, were prepared by literature routes [25–27].

2.2. Calibration of absorption on surface

A drop (0.0045 ml) of a stock solution of $Ni(CO)_2(PPh_3)_2$ (0.0046 g) in CH_2Cl_2 (10 ml) was deposited on the surface of a silicon wafer. The solvent was allowed to evaporate and the FTIR spectrum obtained. This process was repeated yielding the following absorbances for the absorption at 1937 cm^{-1}; 0.0089, 0.015, 0.020, 0.023, 0.028. The area over which the film was deposited was found to be 0.5 cm^2. Each drop of the solution results in an additional coverage of 0.39 molecules per $Å^2$. A calibration curve of absorbance versus molecules/$Å^2$ for the absorbance at 1937 cm^{-1} was made yielding a slope of 0.019 $Å^2$/molecule. Assuming, a molecular volume of approximately 1260 $Å^3$, this corresponds to an absorbance of approximately .00016/monolayer at 1937 cm^{-1}. The corresponding extinction coefficients of the other bands were obtained from the corresponding relative intensity and are presented in Table I.

The electronic absorption spectrum of the film was obtained by transmission spectroscopy from a film spin cast on CaF_2. The FTIR of this film was also obtained and used to calculate the extinction coefficients of the electronic transitions. Results are summarized in Table I.

2.3. Deposition control

A stock solution of $Ni(CO)_2(PPh_3)_2$ (0.0305 g) prepared in methylene chloride (2.0 ml) was prepared. A portion of this solution (0.6 ml) was combined with methylene chloride (0.2 ml) and used to spin coat a silicon chip at a spin rate of 725 RPM. The absorption of this film at 1998 cm^{-1} was found to be 0.0214. This was repeated with the following proportion of stock solution : methylene chloride volumes, 1 : 0, 0.2 : 0.2, 0.2 : 0.4, 0.2 : 0.6. The absorption spectra of each solution was measured yielding absorbances of 0.0259, 0.0149, 0.0089 and 0.0069 for the absorption at 1998 cm^{-1} in order of successive dilution.

TABLE I Electronic and FTIR spectral data for relevant complexes

Complex	Energy (cm^{-1})	ε_{IR} (absorbance/monolayer)	Energy (nm)	ε_{UV} (cm^2/mol)	Assignment
$Ni(CO)_2(PPh_3)_2$	1998	0.00018	290	60.6×10^6	CT
	1937	0.00016			
$Fe(CO)_4(PPh_3)$	2048	0.00047	366	3.78×10^6	d-d
	1973	0.00034	268	34.4×10^6	CT
	1929	0.0011	232	99.3×10^6	CT
$Fe(CO)_3(PPh_3)_2$	1877	0.0010	436	1.12×10^6	d-d
			366	5.77×10^6	d-d
			348	7.69×10^6	d-d
			252	45.0×10^6	CT
			230	72.3×10^6	CT
$Cr(CO)_5PPh_3$	2064	0.00014	366	6.5×10^6	d-d
	1931	0.00038			
	1917	0.00038			

The amount deposited in the films as a function of the spinning speed was also determined. A portion (0.2 ml) of a $Ni(CO)_2(PPh_3)_2$ (0.0402 g) solution prepared in methylene chloride (2.0 ml) was dropped on a silicon chip spinning at 60 RPM. The absorbance of the film associated with the band at 1998 cm^{-1} was measured and found to be 0.295. This procedure was repeated at speeds of 123, 280, 380, 506, 593, 714, 1140, 1788, 2400, 3090 and 4073 RPM yielding films with absorbances for the CO band at 1998 cm^{-1} of 0.236, 0.0478, 0.0614, 0.0414, 0.0472, 0.0476, 0.0382, 0.0320, 0.0291 and 0.0283.

Stock solutions of $Fe(CO)_4(PPh_3)$ (0.0142 g) and $Ni(CO)_2(PPh_3)_2$ (0.0329 g) each in methylene chloride (2 ml each solution) were prepared. A sample (0.2 ml) of the $Fe(CO)_4(PPh_3)$ solution was mixed with a volume of the $Ni(CO)_2(PPh_3)_2$ solution (0.6 ml). A drop of the resultant solution was spin coated onto a silicon wafer at 725 RPM and the FTIR spectrum obtained. This was repeated for the following volumes of the $Fe(CO)_4(PPh_3)$ solution to the $Ni(CO)_2(PPh_3)_2$ solution; 0 : 1, 0.2 : 0.4, 0.2 : 0.2, 0.4 : 0.2, 0.6 : 0.2, 1 : 0. The absorbance of the 1998 cm^{-1} band of the nickel complex and the 2048 cm^{-1} band of the iron complex were, in order of increasing iron content 0.039, 0.030, 0.032, 0.021, 0.013, 0.010 and 0 for the nickel absorption and 0, 0.0085, 0.013, 0.016, 0.020, 0.022, 0.031 for the iron absorption.

2.4. Photolysis of complexes as films on silicon surfaces

All photolysis experiments were done in the same manner. A typical experiment is described herein. A Si(111) surface was coated with a thin amorphous film of $Ni(CO)_2(PPh_3)_2$ by spin coating from a CH_2Cl_2 solution of the precursor. This resulted in the formation of a smooth, uniform coating of the chip. The chip was then transferred to a vacuum dewar, evacuated and the FTIR spectrum obtained. The sample was then irradiated for 30 min. at 366 nm with a light intensity of 3.1 mW/cm^2 and another FTIR spectrum was obtained. This procedure was repeated for the following (accumulated) photolysis times: 65, 90, 120, 240 and 390 min.

The sample was then moved to the Auger spectrometer for elemental analysis of the surface. The results are presented in Table II.

For experiments in which the alloys were fabricated solutions containing both complexes were utilized to coat the chip. Concentrations were adjusted such that the ratio of absorbances allowed for monitoring the concentration of each component of the mixture during photolysis.

2.5. Lithographic patterning from amorphous films of the compounds

A film containing $Ni(CO)_2(PPh_3)_2$ was prepared by spin coating from a methylene chloride solution onto a silicon (111) surface. The sample was placed under a lithography mask held in contact with the surface by gravity. The sample was irradiated with the output of a low pressure mercury lamp for 2 hours. The sample was removed and the surface rinsed with hexane leaving a patterned material.

3. Results and discussion

3.1. Spectroscopic data for the complexes

The FTIR spectrum of the carbonyl regions of the bistriphenylphosphine nickel dicarbonyl is summarized in Table I. The two carbonyl bands observed at 1998 and 1937 cm^{-1} are shifted from the energy determined in solution. In cyclohexane solvent this complex exhibits two bands at 2010 and 1955 cm^{-1} [28]. This shift to lower energy in the film is similar in magnitude to shifts associated with a change in solvation environment [29] and we do not believe this indicates any gross change in the structure of the complex. The absorption bands for thin films of the other complexes are also presented in Table I and have been described previously [15, 17].

The extinction coefficients for the complexes are also included in Table I. These were determined from plots of absorbance vs. amounts of material deposited. Importantly these plots are approximately linear indicating that we can use the absorbance on the surface as an indication of the amount of compound deposited. One other observation concerning the extinction coefficient of the films of the nickel complex was noteworthy. The intensity of the high energy carbonyl stretch at 1998 cm^{-1} was slightly higher than that of the 1937 cm^{-1} band. This relative intensity was reversed in samples prepared by spin coating. Presumably this is related to the different structure of the spin cast film and the films formed by evaporation of solutions. In spite of this variation in the relative intensity the absorbance will be used to monitor the photochemical reactions.

The electronic absorption spectra of the complexes of interest are also presented in Table I. For our purposes the key feature is the existence of absorption bands in

TABLE II Auger analysis of the surfaces formed by the photolysis of amorphous films of the precursors

Precursor film	Sputter time (min)	%Fe	%Cr	%Ni	%P	%C/%O
$Ni(CO)_2(PPh_3)_2$	0			15.5	1.5	75/8
	0.5			22.8	2.9	73/2
	1			21.4	3.1	73/2
	2			22.4	2.6	73/3
	5			24.2	2.6	69/4
$Fe(CO)_4PPh_3$	1	13.1			2.1	74/11
$Cr(CO)_5PPh_3$	1		12.7		3.5	73/10
$Ni(CO)_2(PPh_3)_2/Fe(CO)_4PPh_3$	1	8.0		18.4	3.1	64/6
$Ni(CO)_2(PPh_3)_2/Cr(CO)_5PPh_3$	1		2.4	5.6	7.4	82/2
$Cr(CO)_5PPh_3/Fe(CO)_4PPh_3$	1	11.8	3.2		4.3	73/8

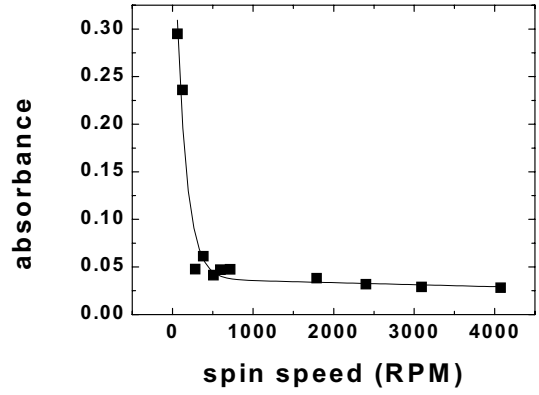

Figure 1 Absorbance associated with the 1937 cm^{-1} band of $Ni(CO)_2(PPh_3)_2$ as a result of spin coating with a 3.14×10^{-2} M solution at various spin speeds.

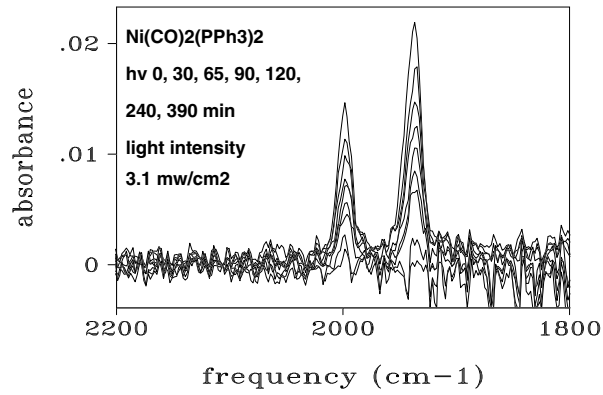

Figure 3 FTIR spectral changes associated with the photolysis of a 100 monolayer film of $Ni(CO)_2(PPh_3)_2$ deposited on Si(111) for 0, 30, 65, 90, 120, 240, and 390 min.

the near UV region for each of these complexes. In addition to the listed bands all these complexes contain charge transfer absorption bands at higher energy.

3.2. Formation of the amorphous $Ni(CO)_2(PPh_3)_2$ films

Thin films of $Ni(CO)_2(PPh_3)_2$ could easily be cast by spin coating from methylene chloride solution. The thickness of the films constructed in this manner was found to be a function of both the spin speed and the concentration of the precursor in the spin coating solution. In Fig. 1 a plot of the absorbance of the film vs. spin speed is shown. This data was generated by spin coating a 3.14×10^{-2} M solution of the nickel precursor. At low spin coating speeds the resultant film is thicker, resulting in a higher absorbance. The film thickness is less reproducible at low spin speeds and the film produced in this fashion may contain crystalline regions. As the spin speed is increased the film absorbance drops rapidly to a plateau region with a small negative incline. Films cast at higher spin speeds were of reproducible thickness and appeared to be of superior optical quality. Similar spin speed profiles have been found to apply to spinning of polymer photoresists [30].

The effect associated with precursor concentration in the spin coating solvent was also investigated. For these experiments a constant spin coating speed of 725 rpm was used to ensure a minimal sensitivity to the spin speed. In Fig. 2 the effect of changing the concentration of $Ni(CO)_2(PPh_3)_2$ in the spin coating solution on the thickness of the final layer is shown. A simple linear relationship between concentration and film thickness is found. This parallels what is often observed in polymer resist spin coating [30].

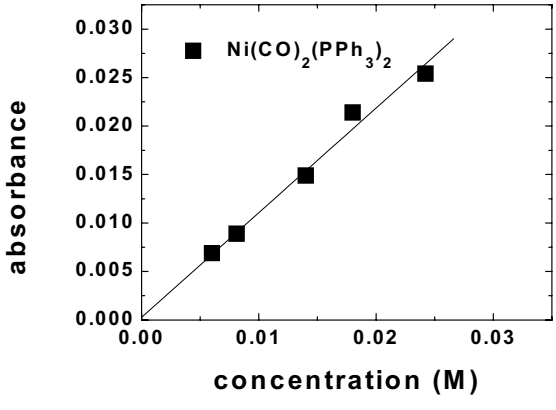

Figure 2 Absorbance associated with the 1937 cm^{-1} band of $Ni(CO)_2(PPh_3)_2$ as a result of spin coating with different concentration solutions at a spin speed of 725 rpm.

3.3. Photochemistry of amorphous films of $Ni(CO)_2(PPh_3)_2$

The spectral changes associated with the photolysis of $Ni(CO)_2(PPh_3)_2$ are depicted in Fig. 3. Photolysis of this complex with 366 nm light resulted in the loss of intensity associated with the carbonyl stretching vibrations. No new transitions, which could be associated with an intermediate, were observed during the decay of the precursor.

This observation is consistent with the photo induced loss of all ligand from this complex and the formation of nickel metal. Apparently a single photon is sufficient to initiate the reaction resulting in the loss of both the carbonyl and phosphine ligands.

Further evidence for this interpretation comes from the analysis of the Auger electron spectrum of the surface following photolysis. The result, presented in Table II, indicate the film is composed of 16% nickel, 75% carbon, 1.5% phosphorus and 8% oxygen. The carbon content at the surface, 75%, exceeds the carbon content of the precursor film and is indicative of surface contamination. Sputtering the surface leads to an observed increase in the observed percentage of phosphorus in the film and a decrease in the amount of oxygen. Presumably this is indicative of a primarily nickel film contaminated with PPh_3. The amount of PPh_3 in the film is consistent with a retention of approximately 7% of the original ligand. The oxygen content is presumably indicative of some nickel oxide formation.

The photochemistry observed is consistent with that shown in Equation 1. The absorption of a photon leads to CO loss generating $Ni(CO)(PPh_3)_2$. This compound is not thermally stable and undergoes thermal decomposition. The CO released both thermally and photochemically from the complex escapes from the film. This is evident from the loss of any absorption attributable to carbon monoxide in the FTIR spectrum following photolysis. The other evidence for the loss of CO from the film is the low signal associated with oxygen that is observed in the Auger electron spectra of the film

following sputtering of the surface. The photogenerated PPh_3 is less able to diffuse out of the film. From the relative nickel and phosphorus signals in the Auger spectra it is apparent that nearly 10% of the ligand remains trapped in the film. It should be noted that the Auger spectrum indicated the formation of some nickel oxide. Presumably the bulk of this oxidation occurred after the sample was removed from the vacuum chamber.

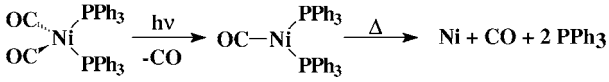

(1)

3.4. Fabrication of amorphous films of mixtures

In order to deposit systems containing more than one metal we must first deposit precursor films composed of multiple precursors. To ensure a homogeneous film is prepared we deposit the film from a single solution containing both precursors. The above photochemistry of the amorphous films does not change the metal composition on the surface hence control of the composition of the amorphous precursor film will allow control of the composition of the resultant product films. In this section the effect of the concentration of the precursor in the spin coating solution on the resultant film composition is investigated. The first question we address if whether the combination of two components in a single precursor solution has an impact on the spin coating of the films.

Precursor solutions containing both components were made and used to coat films under identical conditions. In Fig. 4 the absorbance associated with $Ni(CO)_2(PPh_3)_2$ and $Fe(CO)_4PPh_3$ is correlated with the concentration of each component when they are combined and spun as mixtures. Clearly the amount of each organometallic deposited in the film is proportional to the concentration of that component in the spin coating solution. This indicates that the two components deposit independently of each other. The observed slopes of the absorbance-concentration plots for two components indicate that the efficiency of spin coating of each component is similar. This presumably is a result of similar intermolecular forces between the iron and nickel complexes and their surroundings.

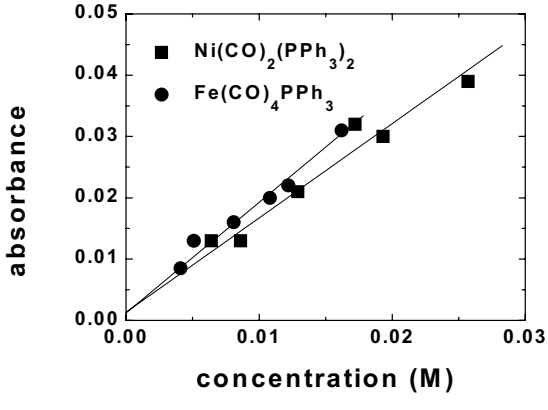

Figure 4 Absorbance associated with the 1937 cm^{-1} band of $Ni(CO)_2(PPh_3)_2$ and the 2048 band of $Fe(CO)_4PPh_3$ as a result of spin coating with different concentration solutions at a spin speed of 725 rpm.

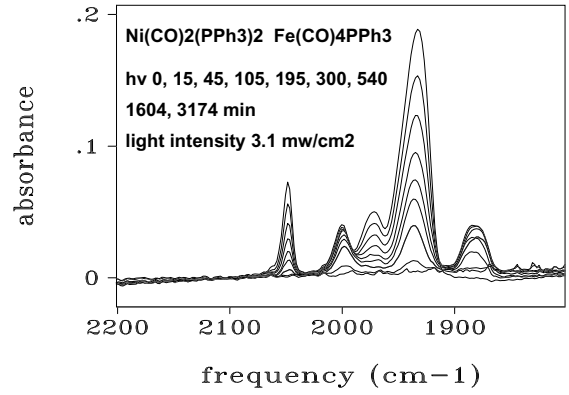

Figure 5 FTIR spectral changes associated with the photolysis of an amorphous film of $Ni(CO)_2(PPh_3)_2$ and $Fe(CO)_4PPh_3$ codeposited on Si(111) 0, 15, 45, 105, 195, 300, 540, 1604, and 3174 min.

Using this procedure films composed of various ratios of $Ni(CO)_2(PPh_3)_2$ and $Fe(CO)_4PPh_3$ and $Cr(CO)_5PPh_3$ could be formed. The photochemistry of these films is described in the following section.

3.5. Photochemical production of films composed of two metals

The spectra associated with the photolysis of the film composed of $Ni(CO)_2(PPh_3)_2$ and $Fe(CO)_4PPh_3$ are shown in Fig. 5. Photolysis results in the loss of spectral features at 1998 and 1937 cm^{-1} and 2048, 1973 and 1929 cm^{-1} associated with $Ni(CO)_2(PPh_3)_2$ and $Fe(CO)_5PPh_3$. The concomitant formation of a single absorption band at 1877 cm^{-1} is also observed. The band at 1887 cm^{-1} reached a maximum intensity following 300 min. photolysis then decays as a result of further photolysis. This band has been observed in the photolysis of $Fe(CO)_4PPh_3$ and is believed to be due to the formation of $Fe(CO)_3(PPh_3)_2$ [15].

The photochemical reaction of $Ni(CO)_2(PPh_3)_2$ appears to be unperturbed by the presence of the $Fe(CO)_4PPh_3$ and proceed according to Equation 1. The photochemistry of the $Fe(CO)_4PPh_3$ proceeds by initial CO loss according to Equation 2. The photoproduct, $Fe(CO)_4PPh_3$, is known to have sufficient thermal stability to associate PPh_3 according to Equation 3 when it is present in the film. In this case the formation of $Fe(CO)_3(PPh_3)_2$ is apparently driven by the PPh_3 released in the photoreaction of the $Ni(CO)_2(PPh_3)_2$. Interestingly the amount of $Fe(CO)_3(PPh_3)_2$ formed is increased in this film over what is found in film composed entirely of the iron precursor [15].

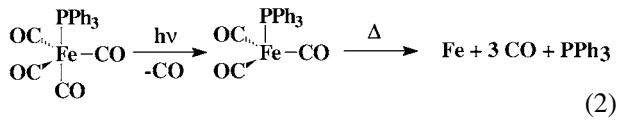

(2)

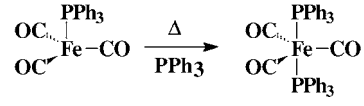

(3)

Auger analysis of the film indicated that sputtering to remove surface contamination yielded a film composed of iron, nickel, phosphorus, carbon and oxygen. The approximate composition assuming the source of

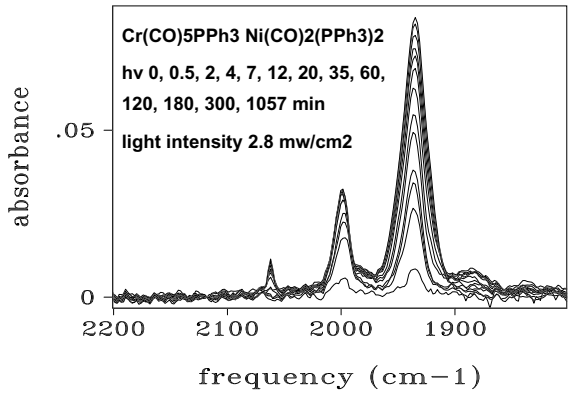

Figure 6 FTIR spectral changes associated with the photolysis of an amorphous film of $Cr(CO)_5PPh_3$ and $Ni(CO)_2(PPh_3)_2$ on Si(111) for 0, 0.5, 2, 4, 7, 12, 20, 35, 60, 120, 180, 300 and 1057 min.

the carbon is entirely PPh_3 ligand can be formulated as $Ni_{18}Fe_8(PPh_3)_{3.1}$. The pure components exhibited a similar level of PPh_3 ligand contamination.

The photochemistry of mixtures of $Ni(CO)_2(PPh_3)_2$ with $Cr(CO)_5PPh_3$ yielded similar results. The spectra associated with the photolysis of a mixture of $Ni(CO)_2(PPh_3)_2$ with $Cr(CO)_5PPh_3$ is shown in Fig. 6. The loss of bands associated with $Ni(CO)_2(PPh_3)_2$ at 1998 and 1937 cm^{-1} and $Cr(CO)_5PPh_3$ at 2064, 1931

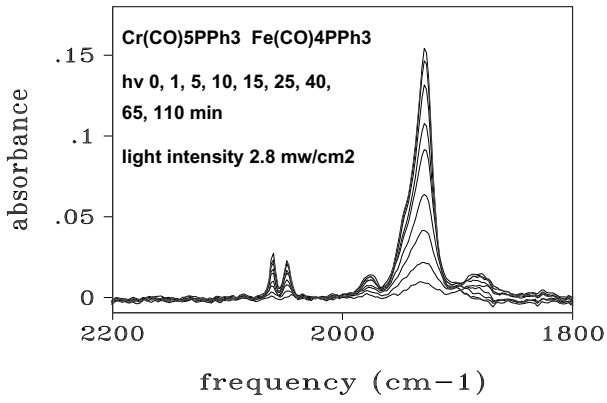

Figure 7 FTIR spectral changes associated with the photolysis of an amorphous film composed of $Cr(CO)_5PPh_3$ and $Fe(CO)_4PPh_3$ on Si(111) for 0, 1, 5, 10, 15, 25, 40, 65, and 110 min.

and 1917 cm^{-1} is apparent. The presence of a weak absorption near 1890 cm^{-1} is evidence for the production of an intermediate during the photoprocess. This intermediate is believed to be associated with the formation of $Cr(CO)_4PPh_3$. Prolonged photolysis of the film results in the loss of intensity from the absorption bands associated with both the nickel and chromium starting materials and the chromium containing intermediate.

The photochemistry is consistent with that described above for both the nickel complex and for the chromium complex [17] as pure films. The photochemistry of the nickel complex is as described above in Equation 1. The photochemistry of the chromium complex is as described in Equation 4. The primary photochemical reaction is the ejection of a single CO from the coordination sphere. The intermediate, $Cr(CO)_4PPh_3$, is itself photosensitive and under continued irradiation decomposes to yield chromium, CO and PPh_3.

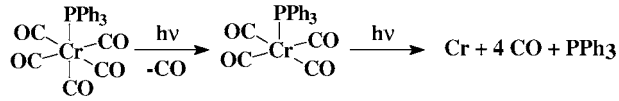

(4)

Auger electron spectra of the photochemically produced films are presented in Table II. Once again the film is may be formulated as a mixture of the two metals and some residual PPh_3. In this case the composition is consistent with $Ni_{5.6}Cr_{2.4}(PPh_3)_{7.4}$.

Finally the photolysis of films composed of both $Cr(CO)_5PPh_3$ and $Fe(CO)_4PPh_3$ was monitored. The results are presented in Fig. 7. Photolysis results in the loss of peaks associated with both $Cr(CO)_5PPh_3$ and $Fe(CO)_4PPh_3$ and an intermediate is apparent below 1900 cm^{-1}. This grows in the early stages of the reaction and reaches a maximum. The continued photolysis results in the loss of this band. This absorption band is consistent with the formation of $Cr(CO)_4PPh_3$ during the reaction although we cannot rule out the possibility that some $Fe(CO)_3(PPh_3)_2$ is also formed. The observations are consistent with the two metal complexes reacting in an independent fashion, each undergoing the thin film photochemistry expected for that species. The

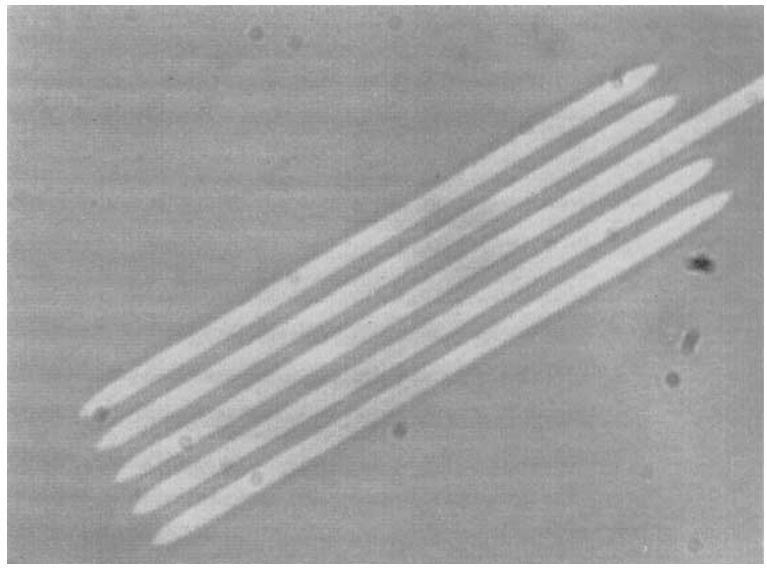

Figure 8 Optical image of lithographed pattern of nickel oxide on a silicon surface. The four lines are 50 μm long providing an internal standard.

results of the Auger electron spectroscopy of the photoproduced films are presented in Table II. The analysis of the film indicates a composition of $Fe_{11.8}Cr_{3.2}(PPh_3)_{4.3}$.

3.6. Lithography

Finally we demonstrate the compatibility of this method to standard lithography procedures by irradiating a sample film of $Ni(CO)_2(PPh_3)_2$ through a standard mask in contact mode. A latent image is visible in the surface following photolysis for one hour. The sample was stable to rinsing with hexane solvent leaving the pattern shown in Fig. 8. In this figure the critical feature size is approximately 2 μm.

Similar experiments have been conducted with the films constructed from mixtures of the compounds. In each case patterned deposits could be constructed by contact lithography from these films. Similar critical feature sizes could be obtained.

4. Conclusions

The photochemical reaction of the $Ni(CO)_2(PPh_3)_2$ led to the production of nickel containing films which retain less than 10% of the phosphine ligand. The deposition of thin films of these organometallic compounds by spin coating follows the general trends found for polymer films. The thickness deposited is directly related to the concentration of the precursor solution and also effected by the spin speed. Importantly the spin coating process can be used to deposit films consisting of two different organometallics. The results contained here also illustrate that this photochemical technique may be used to construct films of different metals. The chemistry of these organometallic precursors is compatible and different precursors may be mixed without causing a change in the photochemistry of the component compounds. In the future we will extend this work to use complexes without the nonvolatile triphenylphosphine ligand. While this ligand was the main source of contamination of the photoproduced film it was a useful in that all the precursors used in this study were reasonably air stable solids.

Acknowledgment

We thank NSERC (CANADA) for financial assistance.

References

1. M. J. ALMOND, D. A. RICE and C. A. YATES, *Chem. in Br.* **24** (1988) 1130.
2. O. ABE and A. TSUGE, *J. Mater. Res.* **6** (1991) 928.
3. M. J. RAND, *J. Electrochem. Soc.* **120** (1973) 686.
4. A. M. DHOTE, S. C. PATIL, S. M. KANETKAR, S. A. GANGAL and S. B. OGALE, *J. Mater. Res* **7** (1992) 1685.
5. R. KUMAR, M. RASHIDI and R. J. PUDDEPHATT, *Polyhedron* **8** (1989) 551.
6. P. SOULETIE and B. W. WESSELS, *J. Mater. Res.* **3** (1988) 740.
7. N. H. DRYDEN, R. KUMAR, E. OU, M. RASHIDI, S. ROY, P. R. NORTON and R. J. PUDDEPHATT, *Chem. Mater.* **3** (1991) 677.
8. H. H. GILGEN, T. CACOURIS, P. S. SHAW, R. R. KRCHNAVEK and R. M. OSGOOD, *Appl. Phys.* B **42** (1987) 55.
9. R. ALEXANDRESCU, E. BORSELLA, S. BOTTI, M. P. CESILE, R. GIORGI, S. MARTELLI, S. TURTU and G. ZAPPA, *J. Mater. Res.* **12** (1997) 774.
10. L. M. FALICOV, D. T. PIERCE, S. D. BADER, R. GRONSKY, K. B. HATHAWAY, H. J. HOPSTER, D. N. LAMBETH, S. S. P. PARKIN, G. PRINZ, M. SALAMON, I. K. SCHULLER and R. H. VICTORA, *ibid.* **5** (1990) 1299.
11. V. P. DRAVID, B. R. ELLIOTT, J. J. HOST, J.-H. HWANG, D. L. JOHNSON, T. O. MASON and M. H. TENG, *ibid.* **12** (1997) 1076.
12. S. VENZKE, R. B. VAN DOVER, J. M. PHILLIPS, E. M. GYORGY, T. SIEGRIST, C.-H. CHEN, D. WERDER, R. M. FLEMING, R. J. FELDER, E. COLEMAN and R. OPILA, *ibid.* **11** (1996) 1187.
13. D. K. LIU, R. J. CHIN and A. L. LAI, *Chem. Mater.* **3** (1991) 13.
14. M. GAO and R. H. HILL, *Journal of Materials Research* **13** (1998) 1397.
15. S. L. BLAIR and R. H. HILL, *J. Organomet. Chem.* **554** (1998) 63.
16. A. BECALSKA, R. J. BATCHELOR, F. W. B. EINSTEIN, R. H. HILL and B. J. PALMER, *Inorg. Chem.* **31** (1992) 3118.
17. C. W. CHU and R. H. HILL *Mater. Chem. and Physics* **43** (1996) 135.
18. D. G. BICKLEY, R. H. HILL and C. I. HORVATH, *J. Photochem. Photobiol. A: Chem.* **67** (1992) 181.
19. C. L. W. CHING and R. H. HILL, *J. Vac. Sci. & Tech.* A. **16** (1998) 897.
20. J. P. BRAVO-VASQUEZ, L. W. C. CHING, W. L. LAW and R. H. HILL, *Journal of Photopolymer Science and Technology* **11** (1998) 589.
21. W. L. LAW and R. H. HILL, *Mater. Res. Bull.* **33** (1998) 69.
22. S. L. BLAIR, J. HUTCHINS, R. H. HILL and D. G. BICKLEY, *J. Mater. Sci.* **28** (1994) 2143.
23. S. L. BLAIR, C. W. CHU, R. DAMMEL and R. H. HILL, in SPIE Proceedings Vol. 3049, Advances in Resist Technology and Processing XIV, edited by G. Regine (1997) p. 829.
24. R. H. HILL and S. L. BLAIR, in Micro and Nano Patterning Polymers, edited by Hiroshi Ito, Elsa Reichmanis, Omkaram Nalamasu, and Takumi Ueno, ACS Symposium Series 706; (1998) ch. 5, p. 53.
25. H. I. CONDER and M. Y. DARENSBURG, *J. Oranomet. Chem.* **67** (1974) 93.
26. F. A. COTTON and R. V. PARISH, *J. Chem. Soc.* (1960) 1440.
27. T. A. MAGEE, C. N. MATTHEWS, T. S. WANG and J. H. WOTIZ, *J. Am. Chem. Soc.* **83** (1961) 3200.
28. L. S. MERIWETHER and M. L. FIENE, *ibid.* **81** (1959) 4200.
29. R. H. HILL and J. D. DEBAD, *Polyhedron* **10** (1991) 1705.
30. D. MEYERHOFER, *J. Appl. Phys.* **49** (1978) 3993.

Received 16 July 2001
and accepted 6 May 2002